

Some properties of synchrotron radio and inverse-Compton gamma-ray images of supernova remnants

O. Petruk^{1,2,4}, V. Beshley², F. Bocchino^{3,4}, S. Orlando^{3,4}

¹*Institute for Applied Problems in Mechanics and Mathematics, Naukova St. 3-b, 79060 Lviv, Ukraine*

²*Astronomical Observatory, National University, Kyryla and Methodia St. 8, 79008 Lviv, Ukraine*

³*INAF - Osservatorio Astronomico di Palermo “G.S. Vaiana”, Piazza del Parlamento 1, 90134 Palermo, Italy*

⁴*Consorzio COMETA, via Santa Sofia 64, 95123 Catania, Italy*

Accepted Received ...; in original form ...

ABSTRACT

The synchrotron radio maps of supernova remnants (SNRs) in uniform interstellar medium and interstellar magnetic field (ISMF) are analysed, allowing different ‘sensitivity’ of injection efficiency to the shock obliquity. The very-high energy γ -ray maps due to inverse Compton process are also synthesized. The properties of images in these different wavelength bands are compared, with particular emphasis on the location of the bright limbs in bilateral SNRs. Recent H.E.S.S. observations of SN 1006 show that the radio and IC γ -ray limbs coincide, and we found that this may happen if: i) injection is isotropic but the variation of the maximum energy of electrons is rather quick to compensate for differences in magnetic field; ii) obliquity dependence of injection (either quasi-parallel or quasi-perpendicular) and the electron maximum energy is strong enough to dominate magnetic field variation. In the latter case, the obliquity dependences of the injection and the maximum energy should not be opposite. We argue that the position of the limbs alone and even their coincidence in radio, X-rays and γ -rays, as it is discovered by H.E.S.S. in SN 1006, cannot be conclusive about the dependence of the electron injection efficiency, the compression/amplification of ISMF and the electron maximum energy on the obliquity angle.

Key words: ISM: supernova remnants – shock waves – ISM: cosmic rays – radiation mechanisms: non-thermal – acceleration of particles

1 INTRODUCTION

The observation of the supernova remnants (SNRs) in very-high energy (VHE) γ -rays by H.E.S.S. and MAGIC experiments is an important step toward understanding the nature of the Galactic cosmic rays and kinematics of charged particles and magnetic field in vicinity of the strong nonrelativistic shocks. However, the spectral analysis of multi-wavelength data allows both for leptonic and hadronic origin of VHE γ -ray emission (e.g. RX J1713.7-3946: Berezhko & Völk (2006), Aharonian et al. (2007)). In this context, the broad-band fitting of the spectrum of the nonthermal emission from SNRs is one of the hot topics in present studies of SNRs. At the same time, another very important source of scientific information, the distribution of the surface brightness, is not in great demand. There are just some discussions emphasizing that observed correlations of brightness in radio, X-rays and γ -rays may be considered to favor electrons to be responsible for VHE emission in RX J1713.7-3946, Vela Jr. and some other SNRs (e.g. Aharonian et al. (2006), Plaga (2008)). However, should the patterns of surface brightness in radio, X-rays and γ -rays

really correlate if the VHE γ -radiation originates from electrons? What should be the limitations for theory once observed patterns are really quite similar, especially in symmetrical bilateral SNRs, like in SN 1006 (H.E.S.S. Source of the Month, August 2008).

Another key issue for particle kinetics is the 3-D morphology of bilateral SNRs in general and SN 1006 particularly. Is it polar-cap or barrel-like? The answer of this question is strongly related to the model of injection (quasi-parallel in the former and isotropic or quasi-perpendicular in the latter case), giving therefore an important hint for acceleration theory. The properties of brightness distribution may be the most conclusive issue in this task (e.g. criterion of Rothenflug et al. (2004), azimuthal profiles comparison in Petruk et al. (2009)).

An experimental investigation of SNR images have to be complemented with theoretical modelling of SNR maps in different energy domains. Radio and X-ray synchrotron images in the uniform interstellar medium (ISM) and the uniform interstellar magnetic field (ISMF) are modeled by Reynolds (1998). The role of gradient of ISM density and

ISMF strength on radio morphology of SNRs are studied by Orlando et al. (2007). These papers bases on the classical MHD and assumes unmodified shocks. Studies on nonthermal images of SNRs with non-linear acceleration theory undergo development (Lee et al. 2008). The profiles of the synchrotron brightness in such SNRs are subject of investigation in Ellison & Cassam-Chenaï (2005) and Cassam-Chenaï et al. (2005).

In the present paper, we present for the first time the inverse-Compton γ -ray images of SNRs in uniform ISM and ISMF produced on the basis of the model of Reynolds (1998). In addition to this model, we allow for different ‘sensitivity’ of injection efficiency to the shock obliquity like it is apparent in numerical results of Ellison et al. (1995). The synthesized maps are compared with the radio ones. Some consequences for origin of VHE emission of SNRs and electron injection scenario are drawn.

2 MODEL

We consider SNR in uniform ISM and uniform ISMF. At the shock, the energy spectrum of electrons is taken as $N(E) = KE^{-s} \exp(-E/E_{\max})$, E_{\max} is the maximum energy of electrons, $s = 2$ is used throughout of this paper. We follow Reynolds (1998) in calculation of the evolution of the magnetic field and relativistic electrons (see details also in Petruk (2006), Petruk & Beshley (2008)). The compression factor for ISMF σ_B increases from unity at parallel shock to 4 at perpendicular one. The fiducial energy at parallel shock, which is responsible for the ‘sensitivity’ of relativistic electrons to the radiative losses (Reynolds 1998) and which is used in IC images is set to E_{\max} . The synchrotron losses are considered as the dominant channel for the radiative losses of relativistic electrons. We assume that K is constant in time; eventual evolution of K affects the radial thickness of rims and does not modify the main features of the surface brightness pattern (Reynolds 1998).

Electrons emitting IC photons have energies $E \sim E_{\max}$. Like K , E_{\max} is assumed to be constant in time. Its possible variation in time does not change the pattern of IC brightness and leads to effects similar to those originating from the time dependence of K . Namely, features in IC images have to be radially thicker if E_{\max} decreases with time (i.e. increases with the shock velocity): since E_{\max} was larger at previous times, there are more electrons in the SNR interior able to emit IC photons at the present time. If E_{\max} increases with time (i.e. decreases with the shock velocity) then maxima in brightness are expected to be radially thinner.

Reynolds (1998) considered three models for injection: quasi-parallel, isotropic and quasi-perpendicular. The pattern of the radio surface brightness distribution in the case of the quasi-perpendicular injection is quite similar to the isotropic injection case, though with different contrasts (Fulbright & Reynolds 1990; Orlando et al. 2007). The numerical calculations of Ellison et al. (1995) show that the obliquity dependence of the injection efficiency ζ (a fraction of accelerated electrons) may be either flatter or steeper than in the classic quasi-parallel case ($\zeta \propto \cos^2 \Theta_o$ where Θ_o is the obliquity angle, the angle between the ISMF and the normal to the shock, Fig. 1). In order to be more general than Reynolds (1998), we allow the injection efficiency to

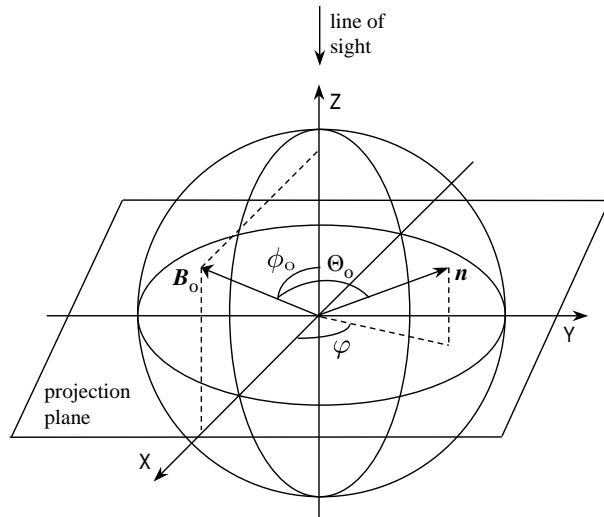


Figure 1. Geometry of the task. The obliquity angle Θ_o , the aspect angle ϕ_o and the azimuth angle φ are shown. ISMF B_o is chosen to be parallel to the X0Z plane.

vary with obliquity angle with different ‘sensitivity’ which is given by the parameter Θ_K :

$$\zeta(\Theta_o) = \zeta_{\parallel} \exp\left(-(\Theta_o/\Theta_K)^2\right) \quad (1)$$

where ζ_{\parallel} is the efficiency for the parallel shock. This expression restores approximately the results of Ellison et al. (1995) with $\Theta_K = \pi/9 \div \pi/4$. The classic quasi-parallel injection may be approximated with $\Theta_K = \pi/6$. Isotropic injection assumes $\Theta_K = \infty$, but the values $\Theta_K \geq 2\pi$ produces almost the same images as $\Theta_K = \infty$ because the range for obliquity angle is $0 \leq \Theta_o \leq \pi/2$.

We consider also quasi-perpendicular injection:

$$\zeta(\Theta_o) = \zeta_{\parallel} \exp\left(-((\Theta_o - \pi/2)/\Theta_K)^2\right). \quad (2)$$

In the most cases presented here, E_{\max} is assumed to be constant over SNR surface; this choice allows us to clearly see the role of other parameters. Reynolds (1998) considered loss-limited, time-limited and escape-limited models for E_{\max} . In all cases, except of the loss-limited one with the level of turbulence comparable with the Bohm limit, E_{\max} should grow with increase of Θ_o (Reynolds 1998). We model the role of possible increase of E_{\max} with obliquity with a simple parameterization

$$E_{\max}(\Theta_o) = E_{\max\parallel} \exp\left(-((\Theta_o - \pi/2)/\Theta_E)^2\right) \quad (3)$$

where Θ_E is a parameter, $E_{\max\parallel}$ the maximum energy at parallel shock. This formula, with different values of Θ_E , is able to restore approximately different cases considered by Reynolds (1998).

The surface brightness is calculated integrating emissivities along the line of sight within SNR. The synchrotron emissivity at some radio frequency is $q_{\text{synch}} \propto KB^{(s+1)/2}$, B is the strength of magnetic field. The γ -ray emissivity of electrons due to inverse Compton process is calculated as

$$q_{\text{ic}}(\varepsilon) = \int_0^{\infty} N(E)p_{\text{ic}}(E, \varepsilon)dE \quad (4)$$

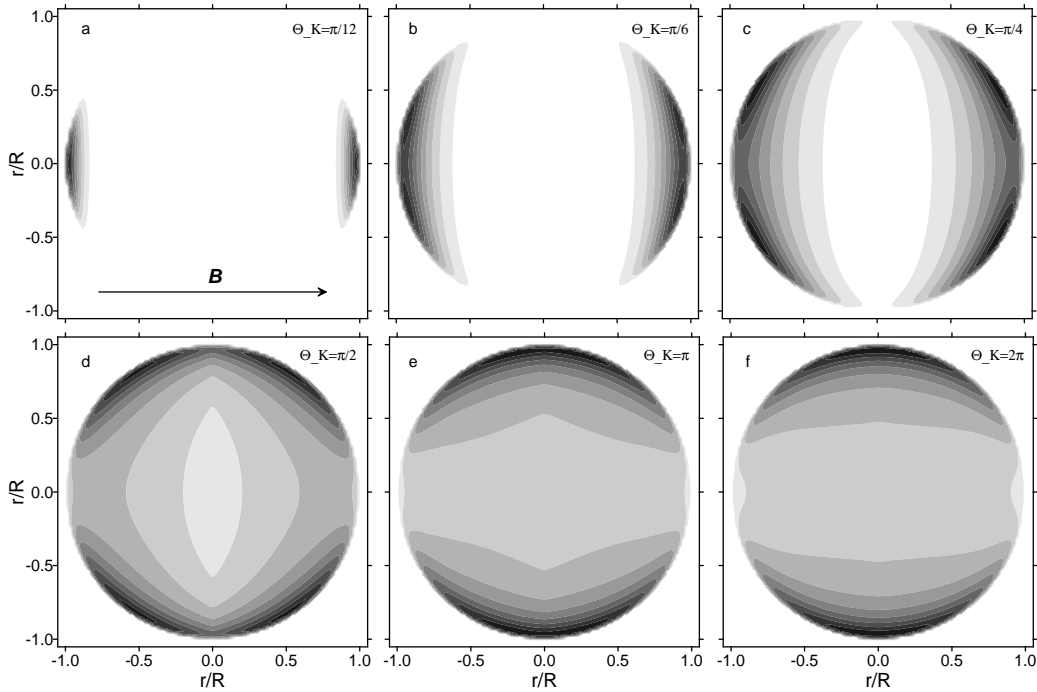


Figure 2. Radio images of SNR for an aspect angle $\phi_o = 90^\circ$ and different Θ_K : $\pi/12$ (a), $\pi/6$ (b), $\pi/4$ (c), $\pi/2$ (d), π (e), 2π (f). Ambient magnetic field is oriented along the horizontal axis. Hereafter, the increment in brightness is $\Delta S = 0.1S_{\max}$.

where ε is the photon energy. The spectral distribution p_{ic} of radiation power of a "single" electron in a black-body photon field with temperature T is

$$p_{ic}(\gamma, \varepsilon) = \frac{2e^4 \epsilon_c}{\pi \hbar^3 c^2} \gamma^{-2} \mathcal{I}_{ic}(\eta_c, \eta_o) \quad (5)$$

where γ is Lorenz factor of electron, $\epsilon_c = kT$,

$$\eta_c = \frac{\epsilon_c \varepsilon}{(m_e c^2)^2}, \quad \eta_o = \frac{\varepsilon^2}{4\gamma m_e c^2 (\gamma m_e c^2 - \varepsilon)}, \quad (6)$$

m_e , e , c , \hbar , k have their typical meaning. $\mathcal{I}_{ic}(\eta_c, \eta_o)$ may be approximated as (Petruk 2008)

$$\mathcal{I}_{ic}(\eta_c, \eta_o) \approx \frac{\pi^2}{6} \eta_c \left(\exp \left[-\frac{5}{4} \left(\frac{\eta_o}{\eta_c} \right)^{1/2} \right] + 2\eta_o \exp \left[-\frac{5}{7} \left(\frac{\eta_o}{\eta_c} \right)^{0.7} \right] \right) \exp \left[-\frac{2\eta_o}{3\eta_c} \right]. \quad (7)$$

This approximation is quite accurate, it represents \mathcal{I}_{ic} in any regime, from Thomson to extreme Klein-Nishina. The maximum of spectral distribution $p_{ic}(\varepsilon)$ for electrons with energy E is at (Petruk 2008)

$$\varepsilon_{\max}(E) \approx \frac{E\Gamma_c}{1 + \Gamma_c}, \quad \Gamma_c = \frac{4\epsilon_c E}{(m_e c^2)^2}. \quad (8)$$

All IC images in the present paper (except of that on Fig. 10) are calculated for the initial photon field with $T = 2.75$ K and for the γ -ray photon energy $\varepsilon = 0.1\varepsilon_{\max}(E_{\max})$ that is for example $\varepsilon = 0.3$ TeV for $E_{\max} = 30$ TeV.

3 RESULTS

3.1 Synchrotron radio images

We stress that all figures in the present paper have been computed using complete MHD model.

Let us define an aspect angle ϕ_o as an angle between interstellar magnetic field and the line of sight (Fig. 1). It is shown that the azimuthal variation of the radio surface brightness S_ϱ at a given radius of projection ϱ , in SNR which is not centrally brightened, is mostly determined by the variations of the magnetic field compression (and/or amplification) σ_B and the electron injection efficiency ς (Petruk et al. 2009):

$$S_\varrho(\varphi) \propto \varsigma(\Theta_{o,\text{eff}}(\varphi, \phi_o)) \sigma_B(\Theta_{o,\text{eff}}(\varphi, \phi_o))^{(s+1)/2} \quad (9)$$

where φ is the azimuthal angle. The effective obliquity angle $\Theta_{o,\text{eff}}$ is related to φ and ϕ_o as

$$\cos \Theta_{o,\text{eff}}(\varphi, \phi_o) = \cos \varphi \sin \phi_o, \quad (10)$$

here, the azimuth angle φ is measured from the direction of ISMF in the plane of the sky (Fig. 1).

Fig. 2 shows how Θ_K affects a radio image of SNR. Complete MHD simulations are in agreement with the approximate formula (9). First, we note that *smooth increase of Θ_K results in transition from the 3-D polar-cap model of SNR to the 3-D barrel-like one*. This is also visible on Fig. 3 where ISMF is directed toward observer. Namely, increase of Θ_K change the visual morphology from centrally-bright to shell-like.

There are three names for a class of SNRs which have two opposite limbs in the literature: 'barrel-shaped' (Kesteven & Caswell 1987), 'bipolar' (Fulbright & Reynolds 1990) and 'bilateral' (Gaensler 1998). They were introduced on the base of 2-D visual morphology. It is interesting that

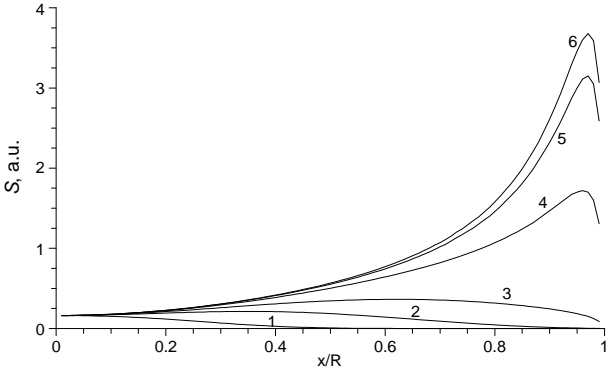


Figure 3. Profiles of the radio surface brightness for an aspect angle $\phi_o = 0^\circ$ (the radial profile of brightness is the same for any azimuth). Θ_K is $\pi/12$ (line 1), $\pi/6$ (line 2), $\pi/4$ (line 3), $\pi/2$ (line 4), π (line 5), 2π (line 6).

the first two names reflects de facto the two different conceptions of SNRs in 3-D.

Fig. 2 also shows that an assumption about orientation of ISMF leads to limitation of possible injection model. Ambient magnetic field in all images on Fig. 2 is along horizontal axis. Thus, *if one consider the polar-cap scenario for bilateral SNR* (ISMF is along axis which crosses two limbs) *then one should consider the injection model which strongly depends on the obliquity* ($\Theta_K \leq \pi/6$, Fig. 2a,b). Instead, *if the barrel is the preferable model* (ISMF is parallel to the symmetry axis between two limbs) *then the injection efficiency should be almost independent of obliquity* ($\Theta_o \geq \pi$, Fig. 2e,f), or prefer quasiperpendicular shocks.

Gaensler (1998) measured the angle ψ between the symmetry axis in 17 ‘clearly’ bilateral SNRs and the Galactic plane. Axes are more or less aligned with the Galactic plane in 12 SNRs ($\psi < 30^\circ$), 2 SNRs have $\psi \approx 45^\circ$ and 3 SNRs is almost perpendicular ($\psi > 60^\circ$). If we assume that ISMF is parallel to the plane of Galaxy then most of bilateral SNRs should be 3-D barrels preferring thus isotropic (or quasiperpendicular) injection.

An interesting feature appears on images for $\Theta_K = \pi/4 \div \pi/2$ (Fig. 2c,d). Namely, SNR has ‘quadrilateral’ morphology. With increasing of obliquity, the injection efficiency decreases while the compression factor of ISMF increases. The variation of injection $\zeta(\Theta_o)$ dominates $\sigma_B(\Theta_o)$ for $\Theta_K \leq \pi/6$. If $\Theta_K \geq \pi$ (injection is almost isotropic) then $\sigma_B(\Theta_o)$ plays the main role in azimuthal variation of the radio surface brightness. In the intermediate range of Θ_K , the significance of the two variations are comparable leading therefore to azimuthal migration of the brightness maxima in the modelled images. There is no ‘quadrilateral’ SNR reported in the literature. If there is no such SNR at all, the range $\Theta_K \simeq \pi/4 \div \pi/2$ may be excluded. However, we stress that a complete statistical study of the morphology of radio SNRs would be needed to definitely assess the lack of quadrilateral SNRs¹.

The visual morphology of SNR is different for different aspect angles. Fig. 4 shows SNR images for quasi-parallel injection with $\Theta_K = \pi/12$ (upper panel) and for isotropic injection ($\Theta_K = 2\pi$, lower panel). We may expect that

ISMF may have different orientation versus observer in various SNRs. If quasi-parallel injection is not a rare exception then the polar-cap SNRs should be projected in a different way and we may expect to observe not only ‘bipolar’ SNRs (Fig. 4c,d) but also SNRs with one or two radio eyes within thermal X-ray rim (Fig. 4a,b). Fulbright & Reynolds (1990) developed statistically this thought and showed that the quasi-parallel injection model would be unlikely, but again, we would need a complete study to verify this statement². Statistical arguments of Fulbright & Reynolds (1990) may be affected by the fact that centrally-bright radio SNRs (lines 1-2 on Fig. 3) are expected to be fainter than bilateral or circular SNRs with the same characteristics (lines 4-6 on Fig. 3); it could be that most of the centrally-peaked SNRs may not be observable.

3.2 IC γ -ray images

Let us consider first the case when the maximum energy of electrons is constant over SNR surface; this allows us to clearly see the role of the injection efficiency and magnetic field variations.

Synthesized IC γ -ray images of SNRs are presented on Fig. 5, for different aspect angles. These images assume almost *isotropic* injection ($\Theta_K = 2\pi$) and should be compared with radio maps on the lower panel of Fig. 4. The component of ISMF which is perpendicular to the line of sight is along horizontal axis on all images. An important difference is prominent from these two figures. Namely, the two lobes develop with increasing of ϕ_o in both radio and γ -rays. However, *their location in respect to ISMF is opposite*. The line connecting two maxima in radio is perpendicular to ISMF while it is parallel to ISMF on IC images (cf. Fig 5d and Fig 4h).

The reason of this effect is the following. For assumed isotropic injection, the azimuthal variation of the radio brightness is determined only by the dependence σ_B on obliquity (the azimuth angle equals to the obliquity angle for $\phi_o = \pi/2$). Electrons emitting VHE γ -rays have energies $E \sim E_{\max}$ and experience substantial radiative losses (this effect is negligible for radio emitting electrons). Magnetic field does not appear directly in the formulae for IC emission, but it affects the downstream distribution of relativistic electrons emitting IC γ -rays. The larger post-shock magnetic field the larger radiative losses. The downstream distribution of IC-emitting electrons is therefore steeper where magnetic field is stronger. This leads to lower IC brightness in SNR regions with larger magnetic field (while radio brightness increases there because of proportionality to $B^{3/2}$).

In VHE γ -ray image of SN 1006 recently reported by H.E.S.S. collaboration (H.E.S.S. Source of the Month, August 2008), the two maxima coincide in location with limbs in radio and nonthermal X-rays. This fact, in view of the ‘limb-inverse’ property, could be considered as argument against the leptonic origin of γ -ray emission in SN 1006 (if injection is isotropic). However, these IC images are obtained under assumption that E_{\max} does not vary over SNR

¹ G338.3-0.0 could be an example of quadrilateral SNR

² G311.5-0.3 and G337.2-0.7 could be examples of SNRs with two radio ‘eyes’

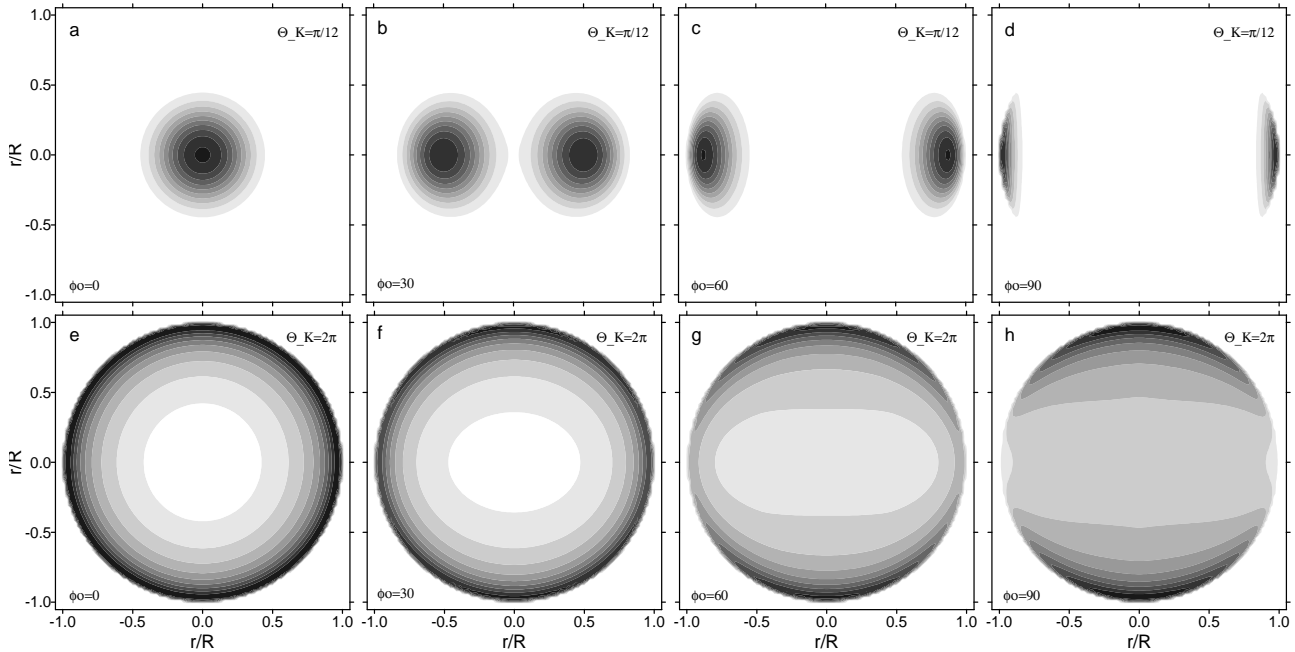


Figure 4. Radio images of SNR for different aspect angles ϕ_o : 0° (a,e), 30° (b,f), 60° (c,g), 90° (d,h). $\Theta_K = \pi/12$ (upper panel), $\Theta_K = 2\pi$ (lower panel). Component of the ambient magnetic field which is perpendicular to the line of sight, is oriented along the horizontal axis.

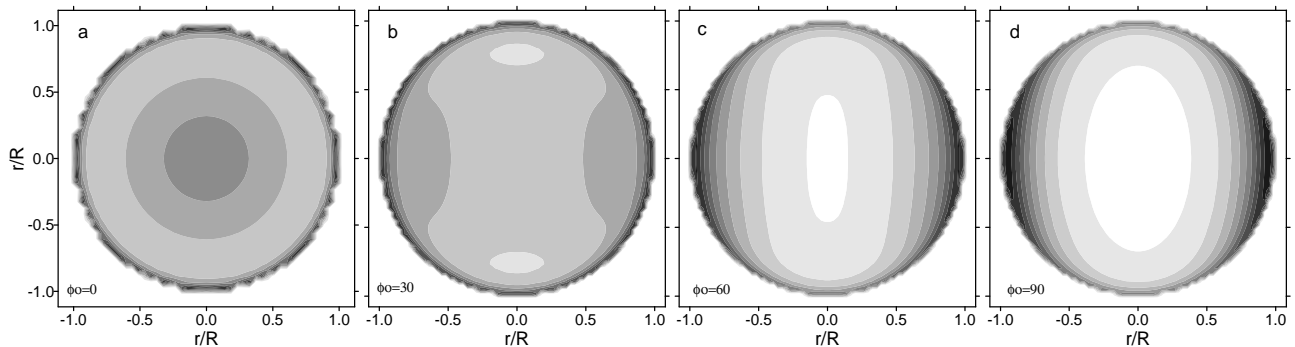


Figure 5. IC γ -ray images of SNR. Isotropic injection, E_{\max} is constant over SNR surface. Aspect angles ϕ_o : 0° (a), 30° (b), 60° (c), 90° (d). Component of the ambient magnetic field which is perpendicular to the line of sight, is oriented along the horizontal axis.

surface. If E_{\max} is high enough at regions with large magnetic field (at perpendicular shock), then the ‘limb-inverse’ effect may be less prominent or even might not be important (see below).

In case if injection strongly prefers *parallel* shocks (limbs in SN 1006 are polar caps), the dependence $\zeta(\Theta_o)$ might dominate $\sigma_B(\Theta_o)$. The maxima of brightness in radio and IC γ -rays are therefore located at the same regions of SNR projection (Fig. 6, to be compared with Fig. 4a,d), in agreement with the Chandra and H.E.S.S. observations of SN 1006.

The role of intermediate values Θ_K for injection which prefers parallel shock, Eq. (1), on profiles of IC brightness is shown on Fig. 7. Increase of the sensitivity of injection to the obliquity leads to radially thinner and more contrast features.

If injection prefers *perpendicular* shock, Eq. (2), its increase in the regions of larger magnetic field may compensate the lack of γ -ray emitting electrons. In that case, the position of limbs coincide in radio and IC γ -rays if the de-

pendence $\zeta(\Theta_o)$ is strong enough (Fig. 8b,d). In the range of intermediate Θ_K , the quadrilateral morphology appears also in models of IC γ -rays (Fig. 8c), as an intermediate morphology between those on Fig. 5d and Fig. 8d. (The contrast of maxima in the image of quadrilateral SNR is so small that this feature may probably not be observable.)

Note that the quasi-perpendicular injection model leads to *radio* images similar to those in the isotropic injection case, cf. Fig. 8a,b and Fig. 2f (see also Orlando et al. (2007)), because magnetic field and injection efficiency increase at perpendicular shocks both leading to larger synchrotron emission. In contrast, there is a lack of IC radiating electrons around perpendicular shocks which may or may not (depending on Θ_K in (2)) compensate it. Thus *IC* images involving the quasi-perpendicular injection may radically differ from those with isotropic injection, cf. Fig. 8d and Fig. 5d.

The obliquity variation of the electron maximum energy is an additional factor affecting the IC γ -ray brightness in

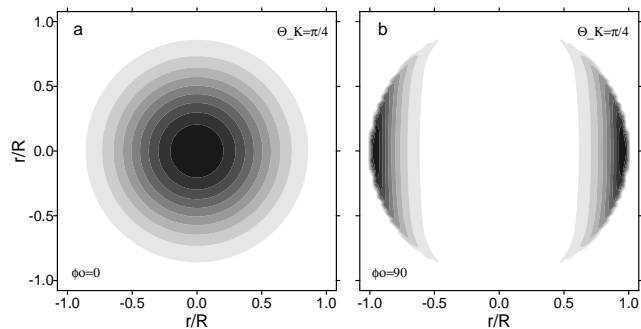


Figure 6. IC γ -ray images of SNR. Quasi-parallel injection (1) with $\Theta_K = \pi/4$, $E_{\max}(\Theta_o) = \text{const}$. Aspect angles ϕ_o : 0° (a), 90° (b). In the latter, ISMF is along the horizontal axis.

SNRs. Actually, Rothenflug et al. (2004) have shown that the cut-off frequency increases at radio limbs of SN 1006 that may (partially) be due to larger E_{\max} there. Therefore E_{\max} is expected to be largest in this SNR at the perpendicular shock (at equatorial belt) if injection is isotropic or quasi-perpendicular or at the parallel shock (at polar caps) if injection is quasi-parallel. In the latter case, the calculations of Reynolds (1998) suggest that the only possible model for E_{\max} in SN 1006 should be loss-limited one in the Bohm limit.

The role of E_{\max} increasing with obliquity, Eq. (3), is shown on Fig. 9. The ‘limb-inverse’ property may not be important and the limbs may coincide in radio, X-rays and IC γ -rays even for the isotropic injection if the maximum energy is large enough at perpendicular shocks to provide energetical electrons in despite of radiative losses (Fig. 9b, cf. with Fig. 4h and Fig. 5d). Note also that the limbs are thicker in this case, because of the more effective radiative losses at perpendicular shock (due to larger ISMF compression), comparing to limbs if they are at parallel shock.

The dependence of E_{\max} on Θ_o may also cause splitting and rotation of IC limbs in case of the quasi-parallel injection (Fig. 9d, cf. with Fig. 6b) or the quasi-perpendicular one. There is a possibility for quadrilateral SNRs to appear in γ -rays due to the interplay between dependences $E_{\max}(\Theta_o)$, $\zeta(\Theta_o)$ and $\sigma_B(\Theta_o)$ (Fig. 9a,d).

All above IC images are calculated for the photon energy $\varepsilon = 0.1\varepsilon_{\max}(E_{\max})$. The pattern of the γ -ray surface brightness remain almost the same with increasing of the photon energy, though regions of maximum brightness become radially thinner and also contrasts change (Fig. 10). This is because electrons which contribute most of emission at larger photon energy experience higher radiative losses and therefore the downstream distribution of these electrons are steeper.

To the end, the main properties of IC surface brightness may simply be derived from the approximate analytical formula for the azimuthal variation of IC surface brightness $S_\varphi(\varphi; \phi_o, \varepsilon)$ of the adiabatic SNR in uniform ISM and uniform ISMF (Appendix):

$$S_\varphi(\varphi) \propto \zeta(\Theta_{o,\text{eff}}) \exp\left(-\frac{E_m \bar{\varrho}^{-1-5\sigma_B(\Theta_{o,\text{eff}})^2 E_m/2E_{f,\parallel}}}{E_{\max,\parallel} \mathcal{F}(\Theta_{o,\text{eff}})}\right) \quad (11)$$

where $E_m \propto \varepsilon^{1/2}$, Eq. (A8), $\bar{\varrho} = \varrho/R \leq 1$, ϱ is the distance from the center of SNR projection. This formula may not be

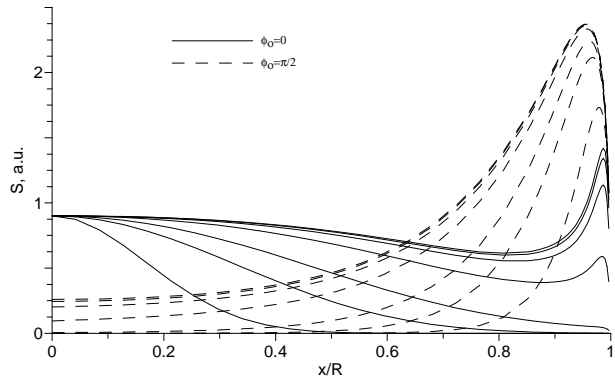


Figure 7. Profiles of the IC surface brightness along X-axis for the aspect angle $\phi_o = 0^\circ$ (the radial profile of brightness is the same for any azimuth; to be compared with Fig. 3) and $\phi_o = 90^\circ$ (ISMF is along the horizontal axis). Dependence of injection is given by (1) with Θ_K (from below): $\pi/12$, $\pi/6$, $\pi/4$, $\pi/2$, π , 2π , ∞ . E_{\max} is constant over SNR surface.

used for SNR which is centrally-bright in γ -rays and is valid for ϱ/R larger than $\simeq 0.9$.

4 CONCLUSIONS

In the present paper, we analyse the synchrotron radio and the inverse-Compton γ -ray images of Sedov SNRs synthesized on the base of the Reynolds (1998) model. Ellison et al. (1995) have shown that the dependence of efficiency of injection ζ on obliquity angle Θ_o may differ from commonly used expression in quasi-parallel case. We therefore parameterise the dependence $\zeta(\Theta_o)$ as it is given by Eq. (1). It is shown that the variation of the parameter Θ_K provide smooth transition from polar-cap ($\Theta_K \leq \pi/6$) to barrel-like ($\Theta_K \geq \pi$) models of SNR and that assumed orientation of ISMF should be related to a certain injection model. Some constraints on injection models which follow from morphological considerations are pointed out. The azimuthal variation of radio brightness is mostly due to variations of ζ and σ_B , in agreement with the approximate formula (9).

Theoretical γ -ray images of SNR due to the inverse Compton effect are reported for the first time. We analyse properties of these images and compare them with corresponding radio maps of SNRs. The azimuthal variation of IC brightness is mostly determined by variations of ζ , σ_B and E_{\max} , in agreement with the approximate formula (11) derived in the Appendix.

In case if E_{\max} is constant over the SNR surface, we found an opposite behaviour of azimuthal variation of surface brightness in radio and IC γ -rays, in case if injection is isotropic and the aspect angle is larger than $\simeq 60^\circ$. Namely, the line crossing the two limbs in radio are perpendicular to the ISMF while they are parallel in IC γ -rays. In particular, bright radio limbs correspond to dark IC areas, in disagreement with X-ray and H.E.S.S. observations of SN 1006. This happens because IC image is affected by large radiative losses of emitting electrons behind perpendicular shock while the larger magnetic field increases the radio brightness there. Variation of E_{\max} over SNR surface may (to some extent) hide this effect. The maximum energy should increase with obliquity in this case.

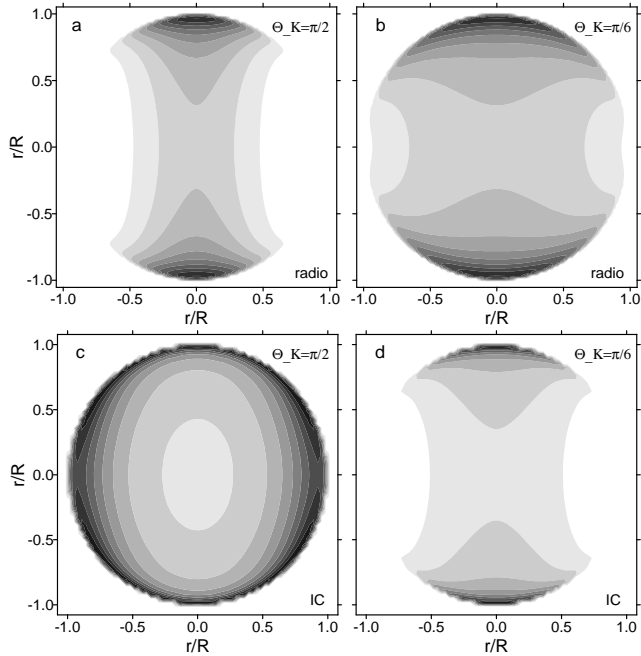


Figure 8. Radio (a,b) and IC γ -ray images (c,d) of SNR for $\phi_o = 90^\circ$. Quasi-perpendicular injection (2) with $\Theta_K = \pi/2$ (a,c) and $\Theta_K = \pi/6$ (b,d) (to be compared with Fig. 4d and Fig. 5d). E_{\max} is constant over SNR surface.

In case of the polar-cap model of SNR (quasi-parallel injection), the maxima in surface brightness are expected to coincide in radio and IC γ -rays (in agreement with H.E.S.S. observation of SN 1006), unless increase of E_{\max} with obliquity will be very strong, which is unlikely in case of SN 1006 because the cut-off frequency is larger at limbs which are at parallel shock in this injection model.

Limbs may also coincide in case of the quasi-perpendicular injection, if the lack of electrons (due to radiative losses) in the regions of large magnetic field is compensated by the strong enough increase of ζ and/or E_{\max} with Θ_o .

Isotropic compression/amplification of ISMF on the shock (i.e. independent of the shock obliquity), like it could be under highly effective acceleration, may also be responsible for the same position of limbs in radio and in IC γ -rays, for the quasi-parallel or quasi-perpendicular injection scenarios. In this case the dependence of $E_{\max}(\Theta_o)$ have to follow variation $\zeta(\Theta_o)$, namely, to be largest (smallest) at parallel shock for quasi-parallel (quasi-perpendicular) injection, otherwise the morphology of SNR in IC γ -rays may differ from the radio one.

We conclude that the location the γ -ray limbs versus radio and X-ray ones, recently discovered by H.E.S.S. in SN 1006, cannot be conclusive about the actual dependence of the electron injection efficiency, the compression/amplification of ISMF and the electron maximum energy on the obliquity angle in this SNR. Detailed features of the SNR maps in different wavebands should be considered for this purpose.

The interplay between dependences $\zeta(\Theta_o)$, $\sigma_B(\Theta_o)$ and $E_{\max}(\Theta_o)$ may cause the quadrilateral morphology in SNR models, due to splitting of maxima in surface brightness.

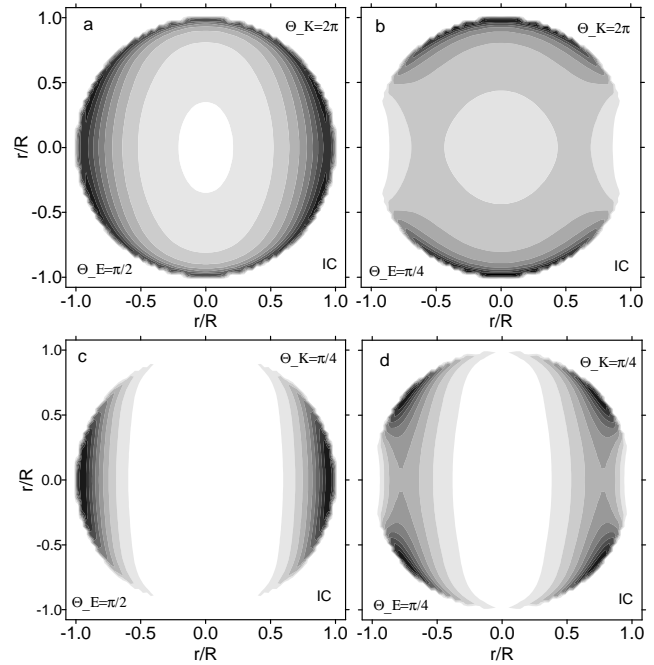


Figure 9. IC γ -ray images of SNR for $\phi_o = 90^\circ$ and E_{\max} increasing with obliquity, Eq. (3) with $\Theta_E = \pi/2$ (a,c) and $\Theta_E = \pi/4$ (b,d). Isotropic injection (a,b), to be compared with Fig. 5d; quasi-parallel injection with $\Theta_K = \pi/4$ (c,d), to be compared with Fig. 6b.

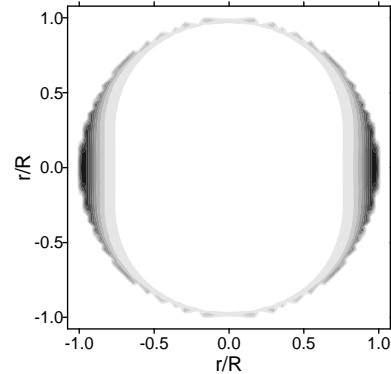


Figure 10. The same as Fig. 5d, for 10 times larger photon energy, $\varepsilon = \varepsilon_{\max}(E_{\max})$.

Absence of quadrilateral SNRs in IC γ -rays, if revealed observationally, may results in limitations on Θ_K and Θ_E .

The detailed characteristics of features on IC image (e.g. thickness of rim) depend on the photon energy. They are radially thinner at larger photon energies, as expected.

ACKNOWLEDGMENTS

OP acknowledge Osservatorio Astronomico di Palermo for hospitality. The work of OP was partially supported by the program 'Kosmofizyka' of National Academy of Sciences (Ukraine). FB, SO and OP acknowledge Consorzio COMETA under the PI2S2 Project, a project co-funded by the Italian Ministry of University and Research (MIUR)

within the Piano Operativo Nazionale ‘Ricerca Scientifica, Sviluppo Tecnologico, Alta Formazione’ (PON 2000-2006).

REFERENCES

- Aharonian, F. et al., 2006, *A&A* 449, 223
 Aharonian, F. et al., 2007, *A&A* 464, 235
 Berezhko, E. G., & Völk, H. J. 2006, *A&A* 451, 981
 Cassam-Chenaï G., Decourchelle A., Ballet J., Ellison D. C., 2005, *A&A* 443, 955
 Ellison D. C., Baring M. G., Jones F. C., 1995 *ApJ*, 453, 873
 Ellison D. & Cassam-Chenaï G., 2005, *ApJ*, 632, 920
 Gaensler B. M., 1998, *ApJ*, 493, 781
 Fulbright M. S., & Reynolds S. P., 1990, *ApJ*, 357, 591,
 Kesteven M. J. & Caswell J. L., 1987, *A&A*, 183, 118
 Lee S.-H., Kamae T., Ellison D. C., 2008, *ApJ*, 686, 325
 Orlando S., Bocchino F., Reale F., Peres G., & Petruk O., 2007, *A&A*, 470, 927,
 Petruk O., 2006 *A&A*, 460, 375
 Petruk O., 2008, *astro-ph/0807.1969*
 Petruk O., Beshley V., 2008, *KPCB*, 24, 159
 Petruk O., Dubner G., Castelletti G., Iakubovskiy D., Kirsch M., Miceli M., Orlando S., Telezhinsky I., 2009, *MNRAS*, accepted
 Plaga R., 2008, *New Astronomy*, 13, 73
 Reynolds S. P., 1998, *ApJ*, 493, 375
 Rothenflug R., Ballet J., Dubner G., Giacani E., Decourchelle A., & Ferrando P., 2004, *A&A*, 425, 121
 Schlickeiser R. *Cosmic Ray Astrophysics* (Springer, 2002)

APPENDIX A: APPROXIMATE ANALYTICAL FORMULA FOR THE AZIMUTHAL VARIATION OF THE IC γ -RAY SURFACE BRIGHTNESS IN SEDOV SNR

An approximate formula for azimuthal variation of the IC γ -ray surface brightness allows one to avoid detailed numerical simulations and may be useful if approximate estimation for the variation is reasonable. It gives deeper insight in the main factors determining the azimuthal behavior of the IC surface brightness in SNRs.

Let the energy of relativistic electrons is E in a given fluid element at present time. Their energy was E_i at the time this element was shocked. These two energies are related as

$$E = E_i \mathcal{E}_{\text{ad}} \mathcal{E}_{\text{rad}} \quad (\text{A1})$$

where \mathcal{E}_{ad} accounts for the adiabatic losses and \mathcal{E}_{rad} for the radiative losses. There are approximations valid close to the shock (Petruk & Beshley 2008):

$$\mathcal{E}_{\text{ad}} \approx \bar{a}, \quad \mathcal{E}_{\text{rad}} \approx \bar{a}^5 \sigma_{\text{B}}^2 E / 2E_{\text{f},\parallel} \quad (\text{A2})$$

where $\bar{a} = a/R$, a is Lagrangian coordinate of the fluid element, $E_{\text{f},\parallel}$ is the fiducial energy for parallel shock. The downstream evolution of K in a Sedov SNR is

$$K \propto \varsigma(\Theta_o) \bar{K}(\bar{a}). \quad (\text{A3})$$

With the approximations (A2), the distribution $N(E)$ may be written in the model of Reynolds (1998) as

$$N(E, \Theta_o) \propto \varsigma(\Theta_o) \bar{K}(\bar{a}) E^{-s} \exp\left(-\frac{E \bar{a}^{-\psi(E, \Theta_o)}}{E_{\text{max},\parallel} \mathcal{F}(\Theta_o)}\right) \quad (\text{A4})$$

where

$$\psi(E, \Theta_o) = 1 + \frac{5\sigma_{\text{B}}(\Theta_o)^2 E}{2E_{\text{f},\parallel}} \quad (\text{A5})$$

and the obliquity variation of the maximum energy of electrons is given by $E_{\text{max}} = E_{\text{max},\parallel} \mathcal{F}(\Theta_o)$.

Electrons with Lorentz factor γ emit most of their IC radiation in photons with energy ε_m . Let us use the ‘delta-function approximation’ (Petruk 2008):

$$p_{\text{ic}}(\gamma, \varepsilon) \approx p_m(\gamma) \delta(\varepsilon - \varepsilon_m), \quad p_m(\gamma) = \int_0^{\infty} p_{\text{ic}}(\gamma, \varepsilon) d\varepsilon. \quad (\text{A6})$$

In the Thomson limit, which is valid for SNRs in most cases, $\varepsilon_m(\gamma) \approx 4kT\gamma^2$ (Petruk 2008) and $p_m(\gamma) = (4/3)c\sigma_{\text{T}}\omega\gamma^2$ (Schlickeiser 2002), T and ω are the temperature and the energy density of initial black-body photons, σ_{T} is the Thomson cross-section.

Substitution (4) with (A6) yields

$$q_{\text{ic}} = \frac{c\sigma_{\text{T}}\omega m_e c^2 \varepsilon^{1/2}}{12\varepsilon_c^{3/2}} N(E_m) \quad (\text{A7})$$

where

$$E_m = \frac{m_e c^2 \varepsilon^{1/2}}{2(kT)^{1/2}} \quad (\text{A8})$$

is the energy of electrons which give maximum contribution to IC emission at photons with energy ε .

Let us consider the azimuthal profile of the IC γ -ray brightness S_ϱ at a given radius ϱ from the centre of the SNR projection.

The obliquity angle Θ_o is different for each radial sector of 3-D object. It is determined, for any position within SNR, by the set $(\varphi, \bar{r}/\varrho, \phi_o)$. Integration along the line of sight gathers information from different radial sectors, with different obliquities. Let us determine the ‘effective’ obliquity angle by the relation

$$\Theta_{o,\text{eff}}(\varphi, \phi_o) = \Theta_o(\varphi, 1, \phi_o). \quad (\text{A9})$$

Actually, $\Theta_{o,\text{eff}}$ for a given azimuth equals to the obliquity angle for a sector with the same azimuth lying in the plane of the sky (i.e. in the plane being perpendicular to the line of sight and containing the center of SNR). Θ_o varies around $\Theta_{o,\text{eff}}$ during integration along the line of sight. The closer ϱ to the edge of SNR projection the smaller the range for variation of Θ_o and more accurate is our approximation.

The surface brightness of SNR projection at distance ϱ from the center and at azimuth φ is

$$S(\bar{\varrho}, \varphi) = 2 \int_{\bar{a}(\bar{\varrho})}^1 q_{\text{ic}}(\bar{a}) \frac{\bar{r} \bar{r}_{\bar{a}} d\bar{a}}{\sqrt{\bar{r}^2 - \bar{\varrho}^2}}, \quad (\text{A10})$$

where $\bar{r}_{\bar{a}}$ is the derivative of $\bar{r}(\bar{a})$ in respect to \bar{a} . The azimuthal variation of the IC brightness for fixed ϱ is approximately

$$\begin{aligned}
 S_\ell &\propto \varsigma(\Theta_{\text{o,eff}}) \exp\left(-\frac{E_m \bar{\varrho}^{-\psi(E_m, \Theta_{\text{o,eff}})}}{E_{\text{max},\parallel} \mathcal{F}(\Theta_{\text{o,eff}})}\right) \\
 &\times \int_{\bar{a}(\bar{\varrho})}^1 \frac{\bar{r} \bar{r}_a d\bar{a}}{\sqrt{\bar{r}^2 - \bar{\varrho}^2}} \exp\left(-\frac{E_m(\bar{a}^{-\psi} - \bar{\varrho}^{-\psi})}{E_{\text{max},\parallel} \mathcal{F}}\right)
 \end{aligned} \tag{A11}$$

If $\bar{\varrho} \rightarrow 1$ then $\bar{a}(\bar{\varrho}) \rightarrow 1$. Thus, the exponent in the integral is roughly unity because $\bar{a}(\bar{\varrho}) \leq \bar{a} \leq 1$ and $\bar{a}(\bar{\varrho}) \leq \bar{\varrho} \leq 1$. The integral in (A11) is therefore roughly the same for any azimuthal angle φ . The azimuthal variation of the IC γ -ray brightness $S_\ell(\varphi; \phi_o, \varepsilon)$ is thus determined mostly just by

$$S_\ell(\varphi) \propto \varsigma(\Theta_{\text{o,eff}}) \exp\left(-\frac{E_m \bar{\varrho}^{-1-5\sigma_{\text{B}}(\Theta_{\text{o,eff}})^2 E_m/2E_{\text{r},\parallel}}}{E_{\text{max},\parallel} \mathcal{F}(\Theta_{\text{o,eff}})}\right) \tag{A12}$$

with E_m given by Eq. (A8), i.e. S_ℓ depends in this approximation on the temperature T of the seed black-body photons and the energy ε of observed γ -photons. The relation between the azimuthal angle φ , the obliquity angle $\Theta_{\text{o,eff}}$ and the aspect angle ϕ_o is as simple as

$$\cos \Theta_{\text{o,eff}}(\varphi, \phi_o) = \cos \varphi \sin \phi_o \tag{A13}$$

for the azimuth angle φ measured from the direction of ISMF in the plane of the sky.

The approximation (A12) may be used for $\bar{\varrho}$ larger than $\simeq 0.9$. Like Eq. (9), Eq. (A12) does not give correct profiles in the case of centrally-bright SNRs, i.e. when $\Theta_{\text{K}} \leq \pi/4$ in (1) and $\phi_o < 30^\circ$.